Supplementary Material

Supplementary material Appendix 1: Infrasound sources and seabird navigation

The following table of infrasound sources has been adapted from the original table compiled by Campus and Christie (2010). The table is based on a literature review of multiple decades of infrasound research and lists a selection of the most commonly observed sources, that are either induced or of natural origin. Many of these sources are routinely observed by the International Monitoring System (IMS) infrasound network, which is in place to monitor infrasound released by nuclear explosion as part of the Comprehensive Nuclear Test-Ban-Treaty (see Appendix 4) and so the listed values for amplitude and frequency content are often recorded, at distances of 100 to 1000 km, and so in the far field. Note that there are potential sources in the marine environment that are not yet fully understood, such as the potential coupling from underwater acoustic energy due to scatter off seamounts and bathymetric features.

For every source, the frequency range, maximum observed amplitude and maximum detection range have been indicated, as well as its temporal characteristics. Note that, while the maximum frequency is listed as 20 Hz, it is likely that these sources may also generate sound at audible frequencies that can be detected at closer distances to the source. Some of the sources are transients and have a finite source time-function, other sources are quasi-continuous. The latter sources typically appear as ambient coherent noise on infrasound sensors and often show temporal variation. For example, this holds for the quasi-continuous noise from glacier calving that grows increasingly strong during the summer when glaciers melt and becomes acoustically active. Similarly, microbarom sources are stronger during the winter when ocean waves are more energetic due to the passage of storms.

The likelihood of seabirds using a particular source is indicated in the last column. This estimate is based on joint evidence from geophysics, physiology and navigational ecology and the reasoning is briefly stated. For the sources that we assert could potentially be used as navigational cues by seabirds, additional information is provided in the table.

Table S1. Overview of infrasound sources and their characteristics, adapted from Campus and Christie (2010). For each source, it is estimated whether seabirds could use this source to navigate, based on evidence listed in the main manuscript. Note that columns 5-9 (marked in italics) have been appended to the original table.

Infrasound source	**Freq. range [Hz]**	**Max. observed amplitude [Pa]**	**Est. max detection range [km]**	***Signal type***	***Origin***	***Source position***	***Temp. variation***	***Likelihood of seabirds using this source to navigate***
Nuclear explosion								
Atmospheric	0.002-20	>20	>20,000	Transient	Induced	Static	N/A	Low; events are not likely to occur.
Underground	1.0-20	~1	~1000	Transient	Induced	Static		
Mining explosion	0.05-20	~5	>5000	Transient	Induced	Static	N/A	Low; rare in the marine environment.
Bridges / structures	~0.5-20	~0.5	<100	Transient	Induced	Static	N/A	Low; far from the marine environment.
Industrial activity	1.0-20	~0.5	~1000	Continuous	Induced	Static	N/A	Low; rare in the marine environment.
Rocket launch	0.01-20	~5	~3000	Transient	Induced	Dynamic	N/A	Low; irregular occurrence. Could disturb flight patterns.
Satellite or	~0.1-10	~1	>2000	Transient	Induced	Dynamic	N/A	Low; irregular occurrence. Could disturb

space-shuttle re-entry								flight patterns.
Subsonic aircraft	0.3-20	~2	<100	Transient	Induced	Dynamic	N/A	Low; irregular occurrence. Could disturb flight patterns.
Supersonic aircraft	0.3-20	~10	~5000	Transient	Induced	Dynamic	N/A	Low; irregular occurrence. Could disturb flight patterns.
Wind turbines	1-10	~0.5	35	Continuous	Induced	Static	N/A	Low; only common in the coastal marine environment.
Meteors	0.001-20	>10	>20,000	Transient	Natural	Dynamic	N/A	Low; events that penetrate into the lower atmosphere occur seldomly. Large events could disturb flight patterns.
Forest fire	2.0-20	~2	~4000	Both	Natural	Static	Annual	Low; too far from the marine environment.
Landslide/ avalanche	~0.1-20	~1	~1000	Transient	Natural	Static	Seasonal	Low; too far from the marine environment.
Waterfalls	0.5-20	~0.2	~200	Continuous	Natural	Static	Seasonal	Low; too far from the marine environment.
Earthquake	~0.005-10	~4	>10,000	Transient	Natural	Static	N/A	Low-intermediate; many events that interact with islands and bathymetry. Coupling remains to be quantified. Large events could disturb flight patterns.

Tsunamis	~0.5-2.0	~0.1	~1000	Transient	Natural	Dynamic	N/A	Low; irregular occurrence and most impact only near coastlines. Large events could disturb flight patterns.
Volcanic eruptions	0.002-20	>20	>20,000	Transient	Natural	Static	N/A	Low-intermediate; Large (distant) events could disturb flight patterns. Coupling from underwater volcanoes remains to be quantified. Note that underwater volcanic activity is often linked with the presence of a rich ecosystem, which could also be feeding places for seabirds.
Mountain associated waves (MAWs)	~0.007 - 0.1	~5	~10,000	Continuous	Natural	Static	Seasonal	Low; sensitivity to signals low due to very low frequencies and amplitudes
Calving glaciers	~0.5-8.0	~1	~200	Transient	Natural	Static	Seasonal	Potential use. Glaciers are continuous sources of infrasound that are always at the same place and provide local information. Land- and sea-terminating glaciers have different spectral characteristics. Signals are confined to a higher frequency range in which sensitivity could be higher.
Lightning	0.5-20	~2	~50	Transient	Natural	Dynamic	Seasonal	Potential use. Thunderstorm activity is concentrated in hotspots around the world due the presence of convective weather patterns, albeit mostly over land and during the spring and summer. High amplitude and wide

								frequency range increases the probability that it could be detected.
Auroral infrasound	0.008-20	~2	~4000	Both	Natural	Dynamic	Diurnal	Potential use. Auroral infrasound can be detected at higher latitudes as near-continuous pulsating signals in a very low frequency band. The signal amplitude and frequency may be too low to be detectable.
Convective storms	0.01-0.1	~0.5	>1500	Both	Natural	Dynamic	Seasonal	Potential use. Storms are dynamic and seasonal and are often constrained in their path, as conditions that are favorable for storm formation occur in certain regions only. Such information could be used by seabirds, either to navigate or to avoid.
Tornadoes / waterspouts	0.5-20	~0.5	~300	Both	Natural	Dynamic	Seasonal	See convective storms
Microbaroms	0.1-1.0	~0.5	~10,000	Continuous	Natural	Dynamic	Daily to seasonal	Potential use. Microbaroms are ubiquitous features of the marine environment. Activity is strongest at high latitudes due to strong ocean wave activity. Low-pressure systems such as hurricanes can lead to rapidly moving microbarom source regions. The signal amplitude and frequency may be too low to be detectable.

Surf	1.0-20	~0.2	~250	Continuous	Natural	Static	Seasonal	Potential use. Surf is continuous and always at the same position, the strength fluctuates with the ocean wave energy. The bathymetric structure around a coastline or island leads to specific surf soundscapes. Hence, surf infrasound could act as a local source of information.

Supplementary Material Appendix 2: Interaural difference cues

Birds can use differences in sound level and timing at their two ears to determine sound source location (Klump, 2000). Because their middle ears are internally coupled by skull spaces and thus act as pressure difference receivers, birds can experience significantly greater interaural differences than are predicted by their typically small heads (Michelsen and Larsen, 2007; Christensen-Dalsgaard, 2011). For pressure difference receivers, eardrum vibration depends on the interaction between an external sound wave reaching the eardrum directly and an internal sound wave that has travelled through the skull. Due to the added sound path through the head, the internal sound wave will differ in amplitude and/or phase relative to the external sound wave.

Principles of Interaural Level Differences (ILD)

For two independent (uncoupled) ears, interaural level differences will only become significant once the frequency is high enough or the head is large enough to cause sound to diffract away from the head (Köppl, 2009). Therefore, level cues would not arise at infrasonic frequencies for bird-sized heads. Pressure difference receiver (coupled) ears can generate interaural level differences at lower frequencies than uncoupled ears. However, mathematical models predict that ILDs are greatest near the frequencies of greatest middle ear vibration (Larsen et al., 2016; Vedurmudi et al., 2016). In birds, this usually occurs at several kHz. Experimental measurement of interaural level differences appear consistent with this expectation (e.g., greater differences at 3 kHz vs 1 kHz for budgerigar *Melopsittacus undulatus*; Larsen et al., 2006). Similarly, in the alligator, a close relative of birds which has similar interaural connections, interaural level differences are ~2 dB re 20µPa at 200 Hz, whereas they are near 6-7 dB re 20µPa at 2.4 kHz (Bierman et al., 2014).

Principles of Interaural Time Differences (ITD)

Analytical models for internally coupled ears (Vedurmudi et al., 2016) and experimental data in birds (Calford and Piddington, 1988; Hyson et al., 1994; Larsen et al., 2006) also indicate interaural time difference enhancements at low frequencies. Interaural time differences boosted by internal coupling are expected to increase and reach a plateau below the frequencies of the greatest middle ear vibration (Vedurmudi et al., 2016), and were indeed observed to increase

towards lower frequencies within the conventional audio range (Fig. S1A; Köppl, 2019). Therefore, ITDs may be of particular use for localizing infrasound sources. In birds, ITDs have been measured that are 3-5 times greater than would be expected based only on head size (i.e. uncoupled ears; Larsen et al., 2006; Carr and Christensen-Dalsgaard, 2015).

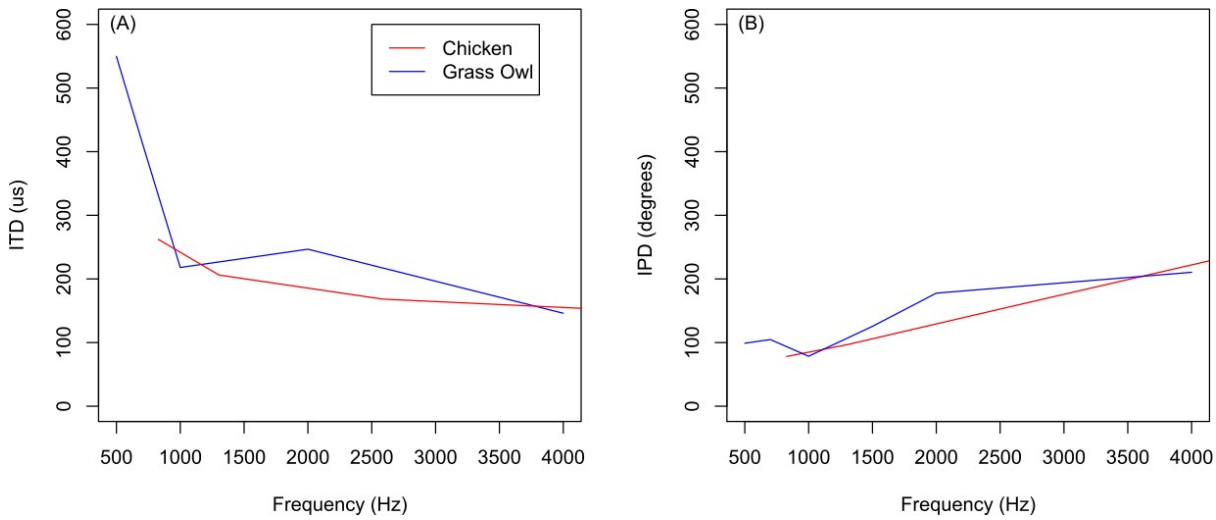

Fig. S1 Interaural Time Differences (ITD) measured using cochlear microphonics (A) and their conversion to Interaural Phase Differences (IPD) (B) [red line = chicken from Hyson et al. (1994); blue line = grass owl from Calford and Piddington (1988)]. As frequency is lowered, greater time differences are required to achieve the same phase difference (phase angle = 360 degrees *ITD*Hz).

However, when expressed in terms of phase differences, there is no increase and there may be even a decrease (Fig. S1B). This is crucial because it is the phase (not time) that is used by the auditory system to encode the signal at each ear and make the binaural comparison in the brain. Low frequencies are encoded by neural firing that follows the phase of the acoustic cycle, known as ‘phase locking’. Neurons from each ear converge on a series of coincidence detectors neurons, which are sensitive to differences in phase between the inputs coming from each ear – these neurons respond maximally when the inputs from each ear are in phase, and minimally when the inputs are 180 degrees out of phase (Ashida and Carr, 2011). Thus, if there is insufficient phase difference between the inputs from each ear, there would be no directional information.

Furthermore, the ability to encode phase information may decrease at very low frequencies (e.g., see Fig. 5b of Schermuly and Klinke, 1990).

What could this mean for infrasound localization by seabirds?

In the absence of experimental data on the interaural differences available to birds at infrasonic frequencies, we can only make informed guesses about the interaural cues available to seabirds: Interaural cues depend both on head size and attenuation of the internal sound path, which can both vary independently across seabird species. Seabirds vary in head size (e.g., skull width of Wilson's storm petrel = 23 mm, skull width of wandering albatross = 75 mm, Zeyl unpublished data). Larger-headed birds are expected to experience greater interaural differences, both ITD (because of longer interaural sound travel distance) and ILD (because of more sound shadowing). On the other hand, larger heads tend to have greater internal attenuation between the ears, reducing the binaural enhancements caused by internal coupling (e.g., Fig. 4 of Calford and Piddington, 1988). Internal attenuation will depend on thickness of tympanic membranes and the cranial pneumaticity that creates the interaural canal. Greater interaural attenuation might be expected in some diving seabirds that have relatively thick, stiff middle ears (e.g., Larsen et al., 2020), or a reduction or loss of the cranial interaural canal connecting the ears (e.g., penguins; Ksepka et al., 2012). However, infrasonic frequencies might be *less* attenuated in the interaural canal than conventional audio frequencies, when there are narrow skull connections. In such cases, propagation could be analogous to propagation in narrow tubes, where sound speed slows down and low frequencies experience less attenuation than higher frequencies (Benade, 1968). Both could contribute to maintaining significant interaural coupling effects at infrasonic frequencies, thus boosting interaural differences.

Supplementary Material Appendix 3: Doppler effect and bird flight

Figure 1 of Quine and Kreithen (1981), which reported the sensitivity of pigeons to frequency shifts at very low frequencies, can be plotted together with the flight speeds that would be required to achieve these frequency shifts:

The required flight speed is calculated using the frequency shift in the Doppler equation and solving for the required flight speed of the receiver. Considering an upward frequency shift, the resulting frequencies that would correspond to the frequency shift thresholds are as follows:

```
f<-f_0*(1+(Threshold/100))
f #frequency shift in Hz

## [1] 1.07  2.08  5.15 10.25 20.20
```

With the frequency shifts associated with those thresholds known, we can rearrange the Doppler equation to calculate the flight speed that is required by the receiver to achieve that frequency shift.

- $(f/f\_0) = ((c+v\_r)/(c+v\_s))$

Assuming the source is not moving, we can rearrange the equation and reduce it to:

- $v\_r = (c*(f/f\_0))-c$

We use the *f* and *f_0* values from the preceding cells to calculate the required flight speeds:

```
Freq_ratio<-f/f_0
Freq_ratio #ratio of frequency shift at threshold to baseline frequency

## [1] 1.070 1.040 1.030 1.025 1.010

v_r = (c*(Freq_ratio))-c
v_r  # flight speed in meters per second

## [1] 23.8 13.6 10.2 8.5  3.4
```

Converting the values from m/s to km/h we get the following:

```
kmph<-v_r*3.6
kmph # flight speed in km/h
```

```
## [1] 85.68 48.96 36.72 30.60 12.24
```

Converting the values from m/s to km/h we get the required flight speeds as they appear in Fig. 2:

```
plot(kmph~f_0, type = "l", ylab = "Flight speed required (km/h)",
    xlab = "Frequency (Hz)")
```

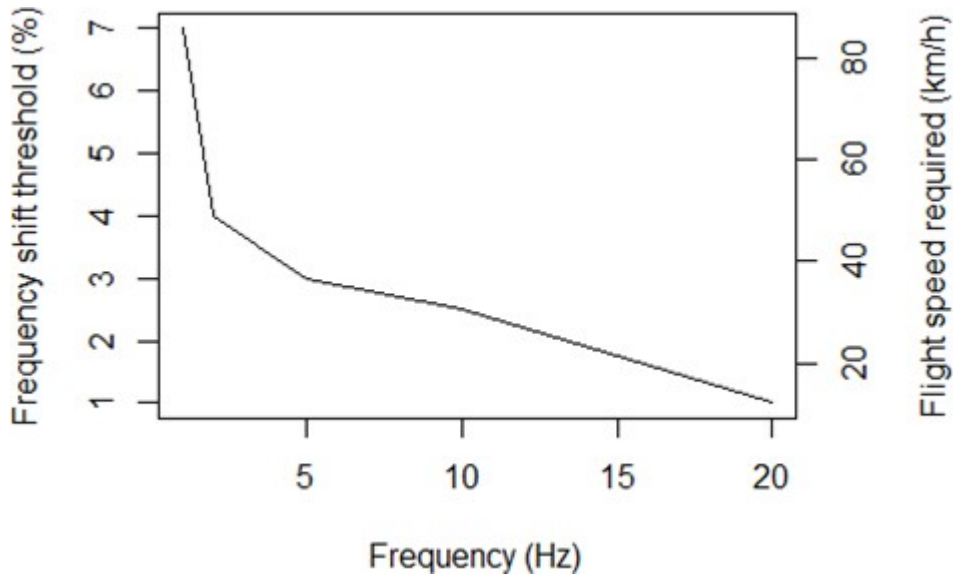

Fig. S2. Experimentally determined thresholds for the detection of frequency shifts in pigeons as a function of frequency [Fig. 1 of Quine and Kreithen (1981)] (left y-axis). The right y-axis shows the corresponding flight speed that would be required to produce an equivalent frequency shift using the Doppler effect.

Supplementary material Appendix 4: Infrasound detections at Kerguelen Island, an IMS array close to the Albatross colony.

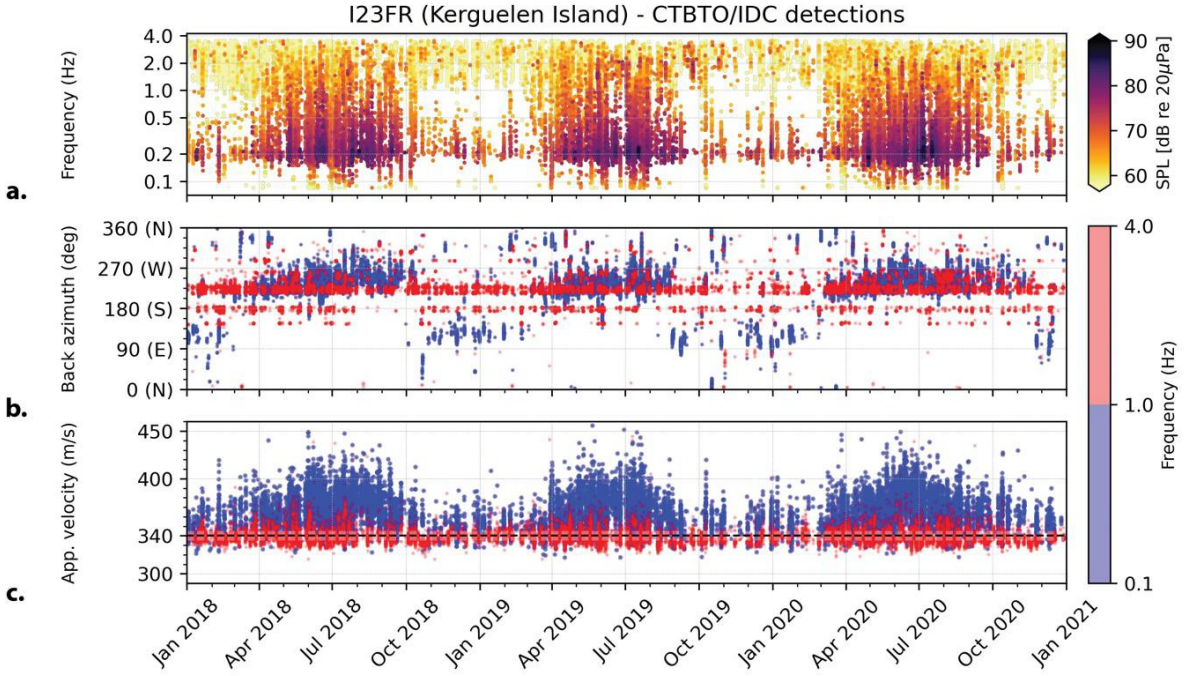

Fig S3A. Example infrasound detection bulletin at Kerguelen Island for the years 2018, 2019 and 2020. The following infrasound wave parameters are plotted as a function of time: (a) centre frequency, (b) back azimuth and (c) apparent velocity. The infrasound detections in frames (b) and (c) have been grouped in two frequency bins, i.e., from 0.1-1 Hz (blue) and from 1-4 Hz (red). While the detections in the high frequency band occur throughout the year, the signals in the low frequency band are mainly detected during the austral winter.

The Kerguelen Islands are a group of islands in the sub-Antarctic, at the intersection of the Indian and the Southern Ocean. The islands are at approximately 1500 km from the colony of Wandering Albatrosses at Crozet Island and is host to IMS infrasound array I23FR. Similar infrasoundscapes are to be expected at both islands, given the close distance and the similarity in environments.

Figure S3A shows the detection of infrasound signals at IMS infrasound array I23FR for the years 2018, 2019 and 2020. The detections are derived from the operational processing database that is maintained by the International Data Centre (IDC) division of the Comprehensive Nuclear-Test-Ban-Treaty Organisation (CTBTO).

The figure illustrates several key aspects of the marine infrasoundscape, including the variation of infrasound detections as a function of time and frequency. The infrasound detections are categorized by (a) centre frequency, (b) back azimuth and (c) apparent velocity.
The back azimuth and apparent velocity quantify the three-dimensional directivity of an infrasound wave. The back azimuth θ is a measure of the horizontal incidence angle and is

defined as the clockwise angle with respect to the north (0 degrees), i.e., east is 90 degrees. The apparent velocity c_{app} relates to the vertical incidence angle ϕ of the sound wave, through the following relation:

$$c_{app} = \frac{c_0}{\cos \phi} \approx \frac{20\sqrt{t + 273}}{\cos \phi}$$

This means that horizontally incident sound waves (for which ϕ = 0°) have apparent velocities that correspond to the local sound speed c_0 (approx. 340 m/s), while sound wave with steeper incidence angles are measured with higher apparent velocities. The vertical incidence angle can be estimated if the local sound speed can be estimated from temperature t (unit °C).

Panel (a) shows the frequency content of the detections for the years 2018, 2019, and 2020. The detections have been coloured as a function of sound pressure level (SPL; expressed in decibel (dB) relative to 20 μPa). Note that the infrasound detections in the frequency band between 0.1-1 Hz have a significant higher SPL compared to the detections in the 1-4 Hz band. The infrasound signals in the 0.1-1 Hz frequency band are to be interpreted as microbaroms, while the signals in the 1-4 Hz band relate to surf (Campus and Christie, 2010). The microbarom signals are centred around 0.2 Hz. To support our interpretation, all infrasound detections have been grouped in these two frequency bands, as shown in panels (b) and (c).

From panel (a) it also follows that the amplitudes of the microbarom signals vary seasonally. The SPL of the microbaroms is higher in winter compared to the summer, which is due to the initial source power of the microbaroms combines with efficient long-range propagation conditions. The increase in source power is related to the higher energetic ocean state during the wintertime. The propagation conditions are influenced by the winds around the stratopause (Figure 2). During the wintertime, the microbarom signals attenuate very little along the propagation path towards the array. In contrast, the surf signals are detected continuously throughout the year, with somewhat higher energy levels during the winter.

Panels (b) and (c) show the direction of arrival and the apparent velocity of microbaroms (blue) and surf (red) as a function of time. Note that both quantities vary significantly with the season. Microbaroms are resolved from the east during the austral summer months, and from the west in winter. The range of detected apparent velocities (i.e., vertical incidence angles) is wider during the austral winter compared to the austral summer periods. This is related to the stronger stratospheric winds during the austral winter (Smets, 2018; Assink et al., 2019).
The resolved surf signals have a constant angle of arrival, and both the SPL and apparent velocity show minor variations as a function of time. This can be understood, as surf infrasound is generated by ocean surface waves colliding on the shore (Figure 2). Because I23FR is an island array, the source location of surf is relatively nearby. Therefore, the infrasound signals of surf do not propagate over large distances (compared to the microbarom signals) and thus are less affected by the atmospheric conditions. The presence of a large bay in the vicinity of I23FR

(i.e., Baie du Morbihan), could partly explain the observations in the surf infrasound band. Due to swell and tides, the bay is a constant generator of surf, which explains the constant direction of the dominant surf direction.

References

Ashida, G., and Carr, C. E. (2011). Sound localization: Jeffress and beyond. *Curr. Opin. Neurobiol.* 21, 745–751. doi:10.1016/j.conb.2011.05.008.

Assink J. et al. (2019) Advances in Infrasonic Remote Sensing Methods. In: Le Pichon A., Blanc E., Hauchecorne A. (eds) Infrasound Monitoring for Atmospheric Studies. Springer, Cham. https://doi.org/10.1007/978-3-319-75140-5_18

Benade, A. H. (1968). On the Propagation of Sound Waves in a Cylindrical Conduit. *J. Acoust. Soc. Am.* 44, 616–623. doi:10.1121/1.1911130.

Bierman, H. S., Thornton, J. L., Jones, H. G., Koka, K., Young, B. A., Brandt, C., et al. (2014). Biophysics of directional hearing in the American alligator (Alligator mississippiensis). *J. Exp. Biol.* 217, 1094–1107. doi:10.1242/jeb.092866.

Calford, M. B., and Piddington, R. W. (1988). Avian interaural canal enhances interaural delay. *J. Comp. Physiol. A* 162, 503–510. doi:10.1007/BF00612515.

Campus, P., and Christie, D. R. (2010). "Worldwide Observations of Infrasonic Waves," in *Infrasound Monitoring for Atmospheric Studies*, eds. A. Le Pichon, E. Blanc, and A. Hauchecorne (Dordrecht: Springer Netherlands), 185–234. doi:10.1007/978-1-4020-9508-5_6.

Carr, C. E., and Christensen-Dalsgaard, J. (2015). Sound Localization Strategies in Three Predators. *Brain. Behav. Evol.* 86, 17–27. doi:10.1159/000435946.

Christensen-Dalsgaard, J. (2011). Vertebrate pressure-gradient receivers. *Hear. Res.* 273, 37–45. doi:10.1016/j.heares.2010.08.007.

Hyson, R. L., Overholt, E. M., and Lippe, W. R. (1994). Cochlear microphonic measurements of interaural time differences in the chick. *Hear. Res.* 81, 109–118. doi:10.1016/0378-5955(94)90158-9.

Klump, G. M. (2000). "Sound Localization in Birds," in *Comparative Hearing: Birds and Reptiles* Springer Handbook of Auditory Research., eds. R. J. Dooling, R. R. Fay, and A. N. Popper (New York, NY: Springer), 249–307. doi:10.1007/978-1-4612-1182-2_6.

Köppl, C. (2009). Evolution of sound localisation in land vertebrates. *Curr. Biol.* 19, R635–R639. doi:10.1016/j.cub.2009.05.035.

Köppl, C. (2019). Internally coupled middle ears enhance the range of interaural time differences heard by the chicken. *J. Exp. Biol.* 222, jeb199232. doi:10.1242/jeb.199232.

Ksepka, D. T., Balanoff, A. M., Walsh, S., Revan, A., and Ho, A. (2012). Evolution of the brain

and sensory organs in Sphenisciformes: new data from the stem penguin Paraptenodytes antarcticus. *Zool. J. Linn. Soc.* 166, 202–219. doi:10.1111/j.1096-3642.2012.00835.x.

Larsen, O. N., Christensen-Dalsgaard, J., and Jensen, K. K. (2016). Role of intracranial cavities in avian directional hearing. *Biol. Cybern.* 110, 319–331. doi:10.1007/s00422-016-0688-4.

Larsen, O. N., Dooling, R. J., and Michelsen, A. (2006). The role of pressure difference reception in the directional hearing of budgerigars (Melopsittacus undulatus). *J. Comp. Physiol. A* 192, 1063–1072. doi:10.1007/s00359-006-0138-1.

Larsen, O. N., Wahlberg, M., and Christensen-Dalsgaard, J. (2020). Amphibious hearing in a diving bird, the great cormorant (Phalacrocorax carbo sinensis). *J. Exp. Biol.* doi:10.1242/jeb.217265.

Michelsen, A., and Larsen, O. N. (2007). Pressure difference receiving ears. *Bioinspir. Biomim.* 3, 011001. doi:10.1088/1748-3182/3/1/011001.

Quine, D. B., and Kreithen, M. L. (1981). Frequency shift discrimination: Can homing pigeons locate infrasounds by Doppler shifts? *J. Comp. Physiol.* 141, 153–155. doi:10.1007/BF01342661.

Schermuly, L., and Klinke, R. (1990). Infrasound sensitive neurones in the pigeon cochlear ganglion. *J. Comp. Physiol. [A]* 166, 355–363.

Smets, P. S. M. (2018). Infrasound and the Dynamical Stratosphere: A new application for operational weather and climate prediction. PhD thesis, Delft University of Technology. doi:10.4233/uuid:517f8597-9c24-4d01-83ed-0f430353e905.

Vedurmudi, A. P., Young, B. A., and van Hemmen, J. L. (2016). Internally coupled ears: mathematical structures and mechanisms underlying ICE. *Biol. Cybern.* 110, 359–382. doi:10.1007/s00422-016-0696-4.